

Simple and Safe Synthesis of Microporous Aluminophosphate Molecular Sieves by Ionothermal Approach

Lijun Han

State Key Laboratory of Multiphase Complex Systems, Institute of Process Engineering,
Chinese Academy of Sciences, Beijing 100080, P.R. China; and
Graduate University of Chinese Academy of Sciences, Beijing 100039,
P.R. China

Yibo Wang

The School of Chemical and Environmental Engineering,
Beijing Technology and Business University, Beijing 100037, P.R. China

Cuixia Li

The School of Chemical and Material Engineering, Southern Yangtze University,
Wuxi, Jiangsu 214122, P.R. China

Suojiang Zhang, Xingmei Lu, and Meijuan Cao

State Key Laboratory of Multiphase Complex Systems, Institute of Process Engineering,
Chinese Academy of Sciences, Beijing 100080, P.R. China

DOI 10.1002/aic.11363

Published online November 13, 2007 in Wiley InterScience (www.interscience.wiley.com).

Pure and transition metal (Co, Fe) containing aluminophosphate molecular sieves were synthesized ionothermally by using a series of imidazolium-based ionic liquids as both solvent and structure-directing agent. Adopting this novel method, a large number of volatile organic solvents can be avoided, and the synthesis can be operated at near atmospheric pressure. Thus, the preparation becomes simple and safe compared with hydrothermal and solvothermal method. And, the recycling of ionic liquid can make the industrial synthesis process more efficient and environmental. The powder XRD patterns and FT-IR spectra displayed that all the synthesized samples were with sodalite structure. Crystal data for Co-substituted analogue: cubic, $Pm\bar{3}n$, $a = 9.0192 \text{ \AA}$ and magnetic property analysis showed weak antiferromagnetic interactions between Co ions. The influences of synthesis conditions such as P_2O_5/Al_2O_3 ratio, crystallization temperature, and the variety of ionic liquids on the character of the products were systematically investigated. In addition, the recycling of ionic liquid was studied based on the NMR and TGA. © 2007 American Institute of Chemical Engineers AICHE J, 54: 280–288, 2008

Keywords: ionic liquid, molecular sieve, SOD, crystallization, recycling

Correspondence concerning this article should be addressed to S. Zhang at sjzhang@home.ipe.ac.cn.

Introduction

Molecular sieve porous materials with special channel or cavity are widely used in many fields such as catalysis, gas adsorption, and separation.^{1–3} The most well-known zeolite molecular sieves are the aluminosilicate zeolites and the microporous silica polymorphs. Since the discovery of aluminophosphates in 1982 by Wilson et al.,⁴ a new family of molecular sieves with rich compositional and structural varieties have been prepared.^{5–8} Especially, the molecular sieves with isomorphous substitution of metal (Cr^{3+} , Co^{2+} , Fe^{3+} , Mg^{2+} , etc.) into framework have been of particular interest over the years because of their redox and catalytic properties in industrial processes.^{9–12}

Traditionally, molecular sieves are synthesized mainly by hydrothermal or solvothermal systems. In those systems, various organic amines or quaternary ammonium were used as structure-directing agents, and vast volatile organic solvents were imported. Also the reactants were placed in a sealed autoclave and heated to 423–473 K resulting in an autogenous pressure. Recently, a novel green method, ionothermal synthesis^{13–19} has been developed for preparing aluminophosphate molecular sieves, using ionic liquids (ILs) as both solvent and structure-directing agent. Generally, ILs, a kind of organic molten salt with melting point below 373 K, have been studied extensively as promising solvent candidates for clean technologies, owing to their special properties such as extremely low vapor pressure, wide liquid range, strong solvent power for organic or inorganic compounds, and high thermal stability.²⁰ Compared with hydrothermal or solvothermal methods, using ionothermal synthesis can avoid the introduction of volatile organic solvents, allow the reactions taking place at near ambient pressure eliminating the safety concerns, and lead to new framework potentially. The essential distinction between this new method and hydrothermal or solvothermal one is that the former relies on the solvent being predominantly ionic, but the latter takes place mainly in molecular solvent. And the most important feature of ionothermal synthesis is the removal of competition between template-framework and solvent-framework interactions which presents in hydrothermal or solvothermal synthesis.¹³ By using this method, some new topological aluminophosphates^{13–17} were synthesized by Morris and coworkers that cannot be prepared from hydrothermal or solvothermal system. Also, Tian and coworkers¹⁸ and Xu et al.¹⁹ studied the effects of amines and microwave heating on ionothermal synthesis of molecular sieves.

The group of materials with sodalite (SOD) structure is very fascinating, because the SOD cage is the basic structural building block of commercially important zeolites A, X, and Y, and has potential technological applications.^{21,22} In previous studies, the microporous aluminophosphate with strong distorted SOD cage (AlPO-SOD) was synthesized in a quasi-nonaqueous medium using dimethylformamide as solvent and template.^{23,24} The pure aluminophosphate and various metal substituted analogues of MIL-74 family $M_3\text{Al}_6(\text{PO}_4)_{12}\cdot 4\text{tren}\cdot 17\text{H}_2\text{O}$ ($M = \text{Na}, \text{Zn}, \text{Fe}, \text{Co}, \text{Mg}, \text{Mn}$) were hydrothermally synthesized using tris(2-aminoethyl)amine (tren) as structure-directing agent.^{25–29} And the magnetic susceptibility of iron(II)-substituted aluminophosphate was measured, which indicated that Fe(II) was not magnetically

coupled in the compound.²⁸ Recently, Parnham and Morris reported the synthesis of cobalt-substituted aluminophosphates using 1-ethyl-3-methyl imidazolium bromide (EmimBr) as both solvent and template.¹⁵ However, it was difficult to prepare pure phase samples in their studies. And previous work on ionothermal synthesis concentrated on a few sorts of ILs. In fact, incorporating transition metal ions into aluminophosphates framework is rarely reported by using ionothermal synthesis.

Therefore, the ionothermal system was chosen in an attempt to explore the application of ILs in the synthesis of metal-substituted aluminophosphates. In this paper, the synthesis of pure and transition metal (Co, Fe) containing microporous aluminophosphates was studied using a series of ILs including 1-ethyl-3-methylimidazolium bromide ([Emim]Br), 1-butyl-3-methylimidazolium bromide ([Bmim]Br), 1-butyl-3-methylimidazolium tetrafluoroborate ([Bmim][BF₄]), and 1-butyl-3-methylimidazolium hexafluorophosphate ([Bmim][PF₆]). The synthesized aluminophosphates were characterized by X-ray single crystal diffraction, powder X-ray diffraction (XRD), scanning electron microscopy (SEM), energy dispersive analysis with X-rays (EDAX), and Fourier transform infrared spectroscopy (FT-IR). The crystal data of Co-substituted analogue displayed that it was cubic, $a = 9.0192 \text{ \AA}$ and described as $\text{Pm}\bar{3}n$. The influences of synthesis conditions on crystallinity of the samples were systematically discussed. Moreover, the recycling of IL and magnetic property of Co-substituted analogue were also studied.

Experimental

Synthesis

A series of imidazolium-based ILs were prepared using standard methods.^{30,31} Simply, *N*-methylimidazole was reacted with a little excess of 1-bromobutane (or bromoethane) in a round-bottom flask at room temperature for 5 h to produce [Bmim]Br (or [Emim]Br). For ILs [Bmim][BF₄] and [Bmim][PF₆], [Bmim]Br was reacted with equal mole of sodium tetrafluoroborate (NaBF_4) or sodium hexafluorophosphate (NaPF_6) in aqueous solution. The obtained ILs were extracted by dichloromethane, and then dried under vacuum at 343 K for 2–3 days before being used.

The typical synthesis procedure of aluminophosphate was as follows¹³: IL, $\text{Al}[\text{OCH}(\text{CH}_3)_2]_3$, H_3PO_4 (85% in H_2O), $\text{CoCl}_2\cdot 6\text{H}_2\text{O}$ or $\text{Fe}(\text{NO}_3)_3\cdot 9\text{H}_2\text{O}$, and HF (40% in H_2O) were added if required to a 23-ml stainless-steel reactor with Teflon liner. The autoclave was heated in an oven to required temperature for several days. Then the autoclave was cooled to room temperature and the product was filtered and washed with ethanol. The filtrate was evaporated to eliminate water and ethanol. Then the concentrated IL was washed with ethyl acetate and dried under vacuum. Therefore, IL can be recycling used. In this paper, pure and Co (Fe)-substituted aluminophosphates were synthesized. Reaction conditions and characters of obtained samples were listed in Table 1.

Characterization

The X-ray single crystal data collection for Co-substituted aluminophosphate was performed on a Bruker Smart 1000 CCD diffractometer, using graphite-monochromated $\text{Mo K}\alpha$

Table 1. Synthesis Conditions and Characters of the Obtained Products

No.	Molar Composition of Reagent	<i>T</i> (K)	Product Characters	Time (d)
1	Al ₂ O ₃ :1.8P ₂ O ₅ :3.6HF:3.0Fe(NO ₃) ₃ ·9H ₂ O:40EmimBr	443	Amorphous phase	5
2	Al ₂ O ₃ :2.0P ₂ O ₅ :3.6HF:3.0Fe(NO ₃) ₃ ·9H ₂ O:40EmimBr	443	Amorphous phase	5
3	Al ₂ O ₃ :2.8P ₂ O ₅ :3.6HF:3.0Fe(NO ₃) ₃ ·9H ₂ O:40EmimBr	443	Brown prolate spheroid	5
4	Al ₂ O ₃ :3.0P ₂ O ₅ :3.6HF:3.0Fe(NO ₃) ₃ ·9H ₂ O:40EmimBr	443	Brown rhombohedron	5
5	Al ₂ O ₃ :5.0P ₂ O ₅ :3.6HF:3.0Fe(NO ₃) ₃ ·9H ₂ O:40EmimBr	443	Brown polyhedron	5
6	Al ₂ O ₃ :6.0P ₂ O ₅ :3.6HF:3.0Fe(NO ₃) ₃ ·9H ₂ O:40EmimBr	443	Amorphous phase	5
7	Al ₂ O ₃ :8.0P ₂ O ₅ :3.6HF:3.0Fe(NO ₃) ₃ ·9H ₂ O:40EmimBr	443	Amorphous phase	5
8	Al ₂ O ₃ :5.0P ₂ O ₅ :3.6HF:3.0CoCl ₂ ·6H ₂ O:40EmimBr	423/433	Amorphous phase	3/5
9	Al ₂ O ₃ :5.0P ₂ O ₅ :3.6HF:3.0CoCl ₂ ·6H ₂ O:40EmimBr	443/453	Blue prolate spheroid	3/5
10	Al ₂ O ₃ :5.0P ₂ O ₅ :3.6HF:3.0CoCl ₂ ·6H ₂ O:40EmimBr	463	Blue rhombohedron	3/5
11	Al ₂ O ₃ :5.0P ₂ O ₅ :3.6HF:3.0CoCl ₂ ·6H ₂ O:40EmimBr	473	Blue prolate spheroid	3
12	Al ₂ O ₃ :3.0P ₂ O ₅ :3.6HF:3.0CoCl ₂ ·6H ₂ O:40 EmimBr	463	Blue rhombohedron	3
13	Al ₂ O ₃ :3.0P ₂ O ₅ :3.6HF:3.0CoCl ₂ ·6H ₂ O:40 BmimBr	463	Blue rhombohedron	3
14	Al ₂ O ₃ :3.0P ₂ O ₅ :3.6HF:3.0CoCl ₂ ·6H ₂ O:40BmimBF ₄	453/463	Blue prolate spheroid	3
15	Al ₂ O ₃ :3.0P ₂ O ₅ :3.6HF:3.0CoCl ₂ ·6H ₂ O:40BmimPF ₆	463	Amorphous phase	5
16	Al ₂ O ₃ :3.0P ₂ O ₅ :3.6HF:40EmimBr (or BmimBr)	463	Colorless transparent rhombohedron	3/5

radiation ($\lambda = 0.71073 \text{ \AA}$). Semiempirical absorption corrections were applied using the SADABS Program. The structure was solved by direct methods and refined by full-matrix least square on F^2 using the SHELXTL-97 program.³² The crystallographic data were listed in Table 2 and atomic coordinates and equivalent isotropic displacement parameters in Table 3. The XRD patterns of synthesized aluminophosphates were recorded on an X'Pert MPD PRO diffractometer (Panalytical) with Cu K α radiation ($\lambda = 1.54059808 \text{ \AA}$).

A JSM-6301F SEM integrated with an EDAX system for elemental analysis was used to confirm the presence of cobalt or iron in the compounds. The morphologies of crystals, observed by SEM, were shown in Figures 1 and 2. FT-IR spectra in the regions ($400\text{--}4000\text{cm}^{-1}$) were recorded by KBr pellet technique using 0.5 mg of sample and 100 mg of KBr on a Thermo Nicolet 380 spectrometer. The thermal gravimetric analysis (TGA) was conducted on a TGA 2050 system from TA Instruments at an advancing heating rate of 10 K/min from 293 to 633 K under N₂, and ¹H NMR spectra were recorded on a BRUKER DPX (400 MHz) in D₂O. Magnetic measurement of Co-substituted aluminophosphate

was performed on Quantum design SQUID MPMS XL magnetometer with a magnetic field of 1000 Oe and operated between 5 and 300 K.

Results and Discussion

Structure analysis

The well-shaped blue rhombdodecahedron of Co-substituted aluminophosphate was synthesized ionothermally by keeping the molar composition to Al₂O₃:5.0P₂O₅:3.6HF:3.0CoCl₂·6H₂O:40[Emim]Br at 463 K for 5 days (Table 1, No. 10). This crystal-shape feature, observed by SEM (Figure 1), was previously reported for the M-aluminum/gallium analogous solids with SOD structure.^{25,28} The crystallographic data were given with cubic crystal system, $a = 9.0192 \text{ \AA}$ and space group $Pm\bar{3}n$ in Table 2. In the framework, aluminum, cobalt, and phosphorus were all in tetrahedral coordination (Figure 3). Owing to the lower Co occupancies of Al sites, the metal tetrahedra were denoted with TO₄ (T = Al or Co). In the compound, PO₄ tetrahedra shared all of their corners with the TO₄ tetrahedra, leading to strict T—O—P alternation. The average T—O and P—O distances in tetrahedra were 1.732 and 1.489 \AA , respectively. The crystal exhibited a three-dimensional SOD framework by connecting the building unit T₂P₂ containing two tetrahedral PO₄ species and two tetrahedral TO₄ ones (Figure 3). The four-member rings and six-member rings were formed by connecting the central atoms of the tetrahedra. A truncated octahedron cage [4⁶6⁸] packed by six 4-member rings and eight 6-member rings were illustrated in Figure 4. The smaller water molecules were embedded in the cages.

Table 3. Atomic Coordinates ($\times 10^4$) and Equivalent Isotropic Displacement Parameters ($\text{\AA}^2 \times 10^3$) for Co-Substituted Crystal

	<i>x</i>	<i>y</i>	<i>z</i>	<i>U</i> (eq)*
P(1)	5000	5000	0	27 (2)
Al(1)	2500	5000	0	21 (2)
Co(1)	2500	5000	0	21 (2)
O(1)	3669 (11)	34,779 (12)	0	109 (8)
O(2)	0	0	0	49 (8)

**U* (eq) is defined as one-third of the trace of the orthogonalized U_{ij} tensor.

Table 2. Crystal Data and Structure Refinement for Co-Substituted Blue Rhombohedron

Empirical formula	H _{0.67} Al _{0.73} Co _{0.27} O _{4.33} P
Formula weight (g mol ^{−1})	136.58
Crystal system	Cubic
Space group	$Pm\bar{3}n$
<i>a</i> (\AA)	9.0192 (8)
α (deg.)	90
<i>Z</i> (calculated density, mg m ^{−3})	6, 1.855
<i>V</i> (\AA^3)	733.68 (11)
Temp (K)	293 (2)
Absorption coefficient (mm ^{−1})	1.473
Reflections collected/unique	3085/155 [<i>R</i> (int) = 0.0288]
λ (Mo K α) (\AA)	0.71073
Final <i>R</i> indices [<i>I</i> > 2 σ (<i>I</i>)]	<i>R</i> ₁ = 0.0980, <i>wR</i> ₂ = 0.2955
<i>R</i> indices (all data)	<i>R</i> ₁ = 0.1001, <i>wR</i> ₂ = 0.2985
Limiting indices	−11 ≤ <i>h</i> ≤ 7, −11 ≤ <i>k</i> ≤ 11, −11 ≤ <i>l</i> ≤ 7
Refinement method	Full-matrix least-squares on F^2
Goodness-of-fit on F^2	1.301

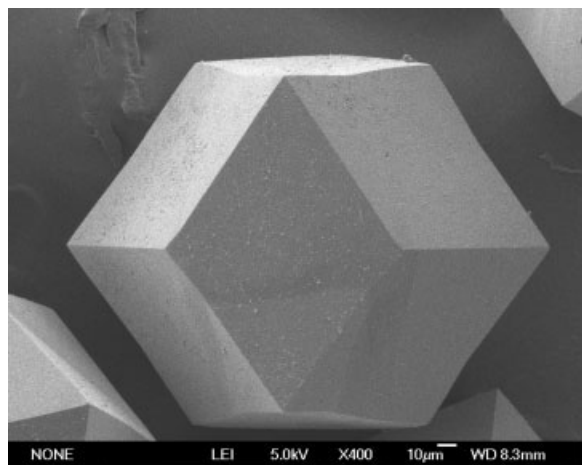


Figure 1. SEM image of AIPO and Co (Fe)-substituted analogues with rhombododecahedron.

Actually, incorporation of transition-metal atoms into aluminophosphate-based zeolite analogue has been succeeded in many systems, but no more than 38% of the Al sites can be replaced.³³ In this crystal, element Co-substituted 27% of Al sites, and the atom ratio of Co/Al is 0.37, [Al + Co]/P is 1 from crystallographic data (measured 0.44 and 0.85 from the EDAX analysis). Figures 5 and 6a showed the powder XRD patterns of Co-substituted analogue from single crystal data and experiment, respectively. As revealed by the identical powder XRD patterns, the synthesized sample obtained by ionothermal method was well crystallized without impure phase.

Fe-substituted aluminophosphates were synthesized with the compositions of $\text{Al}_2\text{O}_3:3\text{P}_2\text{O}_5$ (or $5\text{P}_2\text{O}_5$):3.6HF:3.0Fe(NO_3):9 H_2O :40[Emim]Br at 443 K for 5 days (Table 1, Nos. 4–5). The SEM images of the samples with brown rhombododecahedron and polyhedron were shown in Figures 1 and 2, respectively. At the very similar compositions without addition of any metal (Table 1, No. 16), the pure aluminophosphate (AIPO) with colorless transparent rhombododecahedron was obtained too. The powder XRD patterns of AIPO

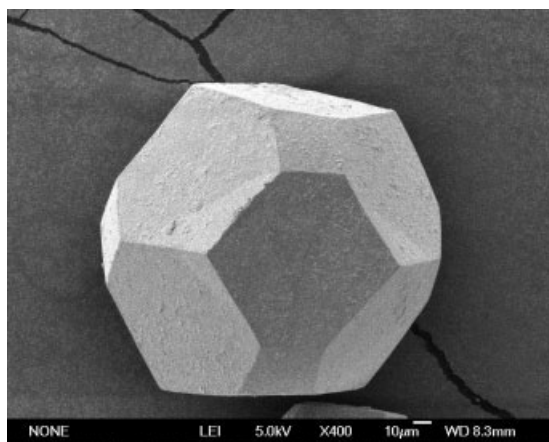


Figure 2. SEM image of Fe-substituted analogue with polyhedron.

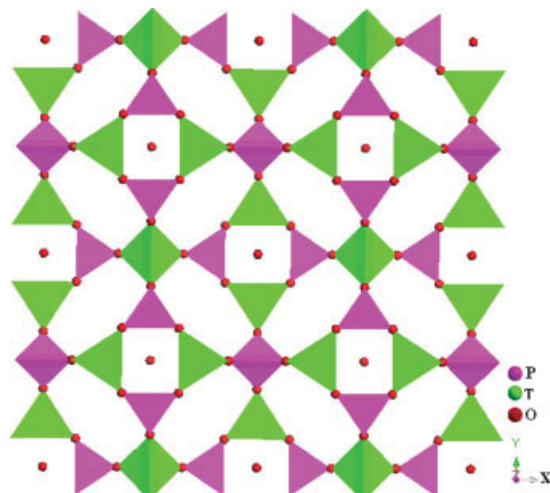


Figure 3. Polyhedral view of $[\text{TO}_4]$ and $[\text{PO}_4]$ in Co-substituted analogue.

[Color figure can be viewed in the online issue, which is available at www.interscience.wiley.com.]

and Fe-substituted analogues were shown in Figures 6b–d. From Figure 6, it was observed that all the powder XRD patterns were in accordance with the simulated powder XRD of Co-substituted analogue, which indicated that all the products were with pure SOD phase. In the Fe-substituted analogues, molar ratios of Fe/Al were 0.62, 0.47, and those of $[\text{Fe}+\text{Al}]/\text{P}$ were 0.81:1 and 0.85:1 from EDAX, respectively. Different Fe/Al ratios indicated that the element iron substituted the sites of Al at different extents. And the molar ratios of $[\text{Fe}+\text{Al}]/\text{P}$ were almost equal to that of $[\text{Co}+\text{Al}]/\text{P}$, namely M/P ($\text{M} = \text{Fe}+\text{Al}, \text{Co}+\text{Al}$) ratios were identical in the different compounds, which showed that all of them adopted metal substituting for Al mechanism.³⁴

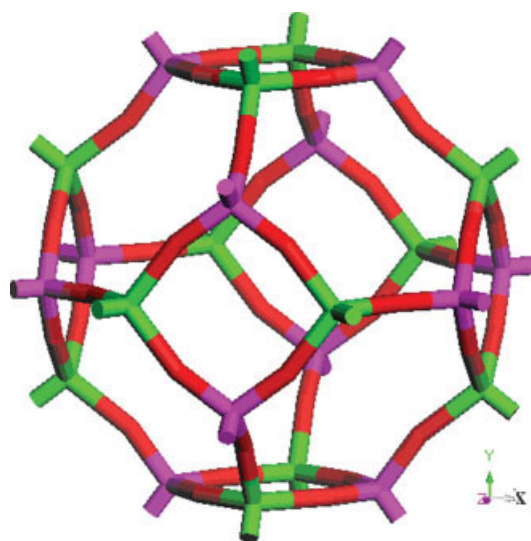


Figure 4. The cage $[4^6 6^8]$ of Co-substituted analogue.

[Color figure can be viewed in the online issue, which is available at www.interscience.wiley.com.]

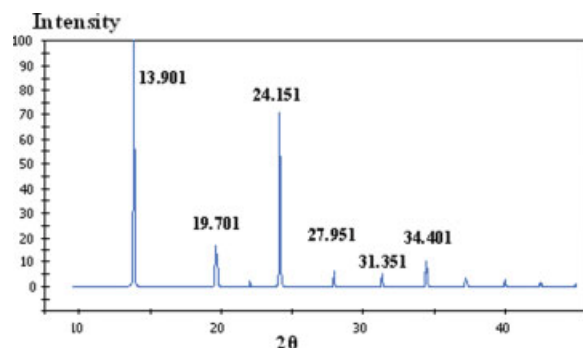


Figure 5. Powder XRD pattern simulated from single crystal structure data of Co-substituted analogue.

[Color figure can be viewed in the online issue, which is available at www.interscience.wiley.com.]

The FT-IR spectra of AlPO and Co (Fe)-substituted analogues with SOD were displayed in Figure 7. Generally, absorptions below 1400 cm^{-1} are attributed to the lattice vibration of molecular sieve framework. As described in Figure 7a, for the as-synthesized AlPO, bands at 1489.29 cm^{-1} could be assigned to the bending vibrations of O—H. Absorptions at 1070.89 cm^{-1} and 722.83 cm^{-1} were referred to internal asymmetrical and symmetrical stretching vibrations of AlO_4 and PO_4 tetrahedra. Additionally, two bands at 624.70 cm^{-1} and 572.07 cm^{-1} were due to the distortion vibrations of four-membered ring and six-membered ring. The band at 485.55 cm^{-1} was attributed to the bending vibration of Al—O. The Co (Fe)-substituted compounds exhibited similar patterns of IR spectra in Figures 7b–c, and the band shift was observed due to the incorporation of cobalt or iron. Those results were consistent with previous studies^{35–38} and further proved that the three compounds were with the same structure.

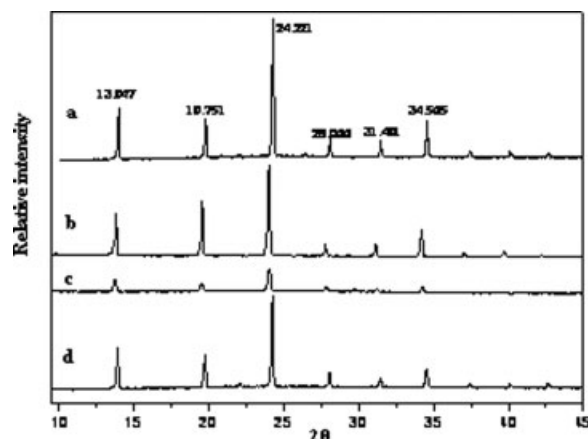


Figure 6. Powder XRD patterns of the samples: (a) Co-substituted analogue; (b) pure aluminophosphate; (c) Fe-substituted analogue with rhombohedron; (d) Fe-substituted analogue with polyhedron.

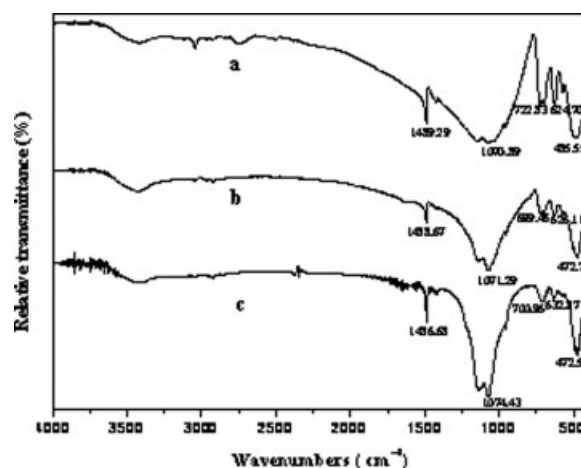


Figure 7. FT-IR spectra of the samples: (a) as-synthesized aluminophosphate; (b) Co-substituted analogue; (c) Fe-substituted analogue.

Effects of synthesis conditions on crystallinity of the aluminophosphates

A series of experiments were operated to investigate the influences of synthesis conditions on product crystallinity, including the mainly factors such as $\text{P}_2\text{O}_5/\text{Al}_2\text{O}_3$ ratio, crystallization temperature, and the type of IL. And the synthesis conditions were listed in Table 1.

In order to investigate the effect of $\text{P}_2\text{O}_5/\text{Al}_2\text{O}_3$ ratio, molar compositions of $\text{Al}_2\text{O}_3 \cdot x\text{P}_2\text{O}_5 \cdot 3.6\text{HF} \cdot 3.0\text{Fe}(\text{NO}_3)_3 \cdot 9\text{H}_2\text{O} : 40[\text{Emim}]\text{Br}$ ($x = 1.8\text{--}8$) were analyzed at 443 K for 5 days (Table 1, Nos. 1–7). As displayed in Figure 8, the crystallinity increased initially with the increase of $\text{P}_2\text{O}_5/\text{Al}_2\text{O}_3$ ratio, and perfect Fe-substituted crystals were obtained at the $\text{P}_2\text{O}_5/\text{Al}_2\text{O}_3$ ratios of 3:1 and 5:1. But with the increase of $\text{P}_2\text{O}_5/\text{Al}_2\text{O}_3$ ratio, the crystallinity decreased and amorphous phase was formed at the $\text{P}_2\text{O}_5/\text{Al}_2\text{O}_3$ ratio of 6:1. According to the change of the crystallinity, we attributed the reason of crystal deterioration to the improper pH value. Generally, the crystallization of the molecular sieves was mostly influenced by the pH of

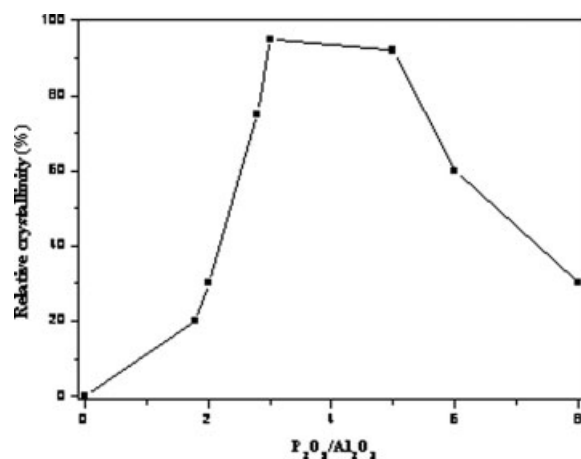


Figure 8. Effect of $\text{P}_2\text{O}_5/\text{Al}_2\text{O}_3$ ratio on relative crystallinity of Fe-substituted analogue.

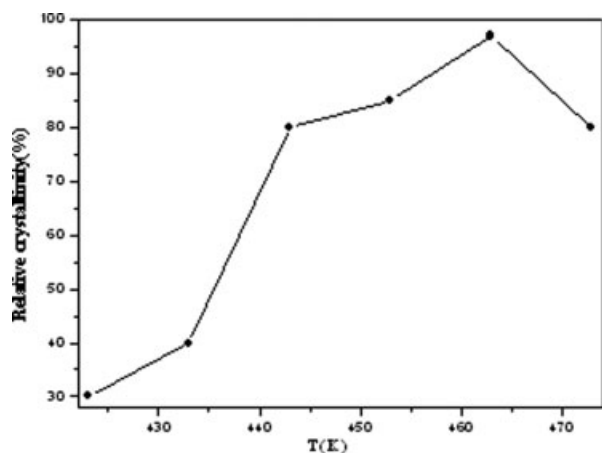


Figure 9. Effect of crystallization temperature on relative crystallinity of Co-substituted analogue.

reaction system.^{39,40} And the acidity of reaction composition was mainly decided by the content of H_3PO_4 , while keeping HF acid constant. As we knew, the concentration of H_3PO_4 controlled the hydrolyzing rate of aluminium triisopropoxide and affected the formation of Al—O—P chains and the primary units of the molecular sieve. But excessive H_3PO_4 would introduce larger quantities of water, which would affect the ionothermal condition. Therefore, there existed an optimum $\text{P}_2\text{O}_5/\text{Al}_2\text{O}_3$ ratio for the formation of perfect crystals. The

aforementioned analysis indicated that a slightly lower concentration of orthophosphoric acid was favorable to grow well-shaped crystals.

The influence of reaction temperature on the crystallinity was studied by keeping the starting composition to $\text{Al}_2\text{O}_3:5.0\text{P}_2\text{O}_5:3.6\text{HF}:3.0\text{CoCl}_2\cdot 6\text{H}_2\text{O}:40[\text{Emim}]\text{Br}$ from 423 to 473 K, with the interval of 10 K for 3 days (Table 1, Nos. 8–11). As seen in Figure 9, the crystallinity was very low, and an amorphous phase appeared at 423 K. When increasing reaction temperature, the crystallinity increased and perfect blue rhombododecahedron morphology was obtained at 463 K. With the increase of temperature, the crystallinity decreased and prolate spheroid was formed at 473 K. These results suggested that higher reaction temperature was beneficial to the crystal formation reaching the optimum at 463 K. It was attributed to the lower viscosity of IL and higher growth ratio of crystal at higher temperature.

In the experiments, the synthesis of Co-substituted aluminophosphate was studied at the composition of $\text{Al}_2\text{O}_3:3.0\text{P}_2\text{O}_5:3.6\text{HF}:3.0\text{CoCl}_2\cdot 6\text{H}_2\text{O}:40\text{IL}$. ILs were used including $[\text{Emim}]\text{Br}$, $[\text{Bmim}]\text{Br}$, $[\text{Bmim}][\text{BF}_4]$, and $[\text{Bmim}][\text{PF}_6]$ (Table 1, Nos. 12–15). Under the similar condition, the Co-substituted analogue was formed in ILs $[\text{Emim}]\text{Br}$, $[\text{Bmim}]\text{Br}$, or $[\text{Bmim}][\text{BF}_4]$, but not in $[\text{Bmim}][\text{PF}_6]$. That may be due to the special property of $[\text{Bmim}][\text{PF}_6]$ IL. Generally, ILs $[\text{Emim}]\text{Br}$, $[\text{Bmim}]\text{Br}$ and $[\text{Bmim}][\text{BF}_4]$ are hydrophilic, but ILs containing $[\text{PF}_6]^-$ anion are hydrophobic. Moreover, $[\text{PF}_6]^-$ undergoes hydrolysis easily to produce HF and $[\text{PO}_4]^{3-}$ in the presence of a small quantity of

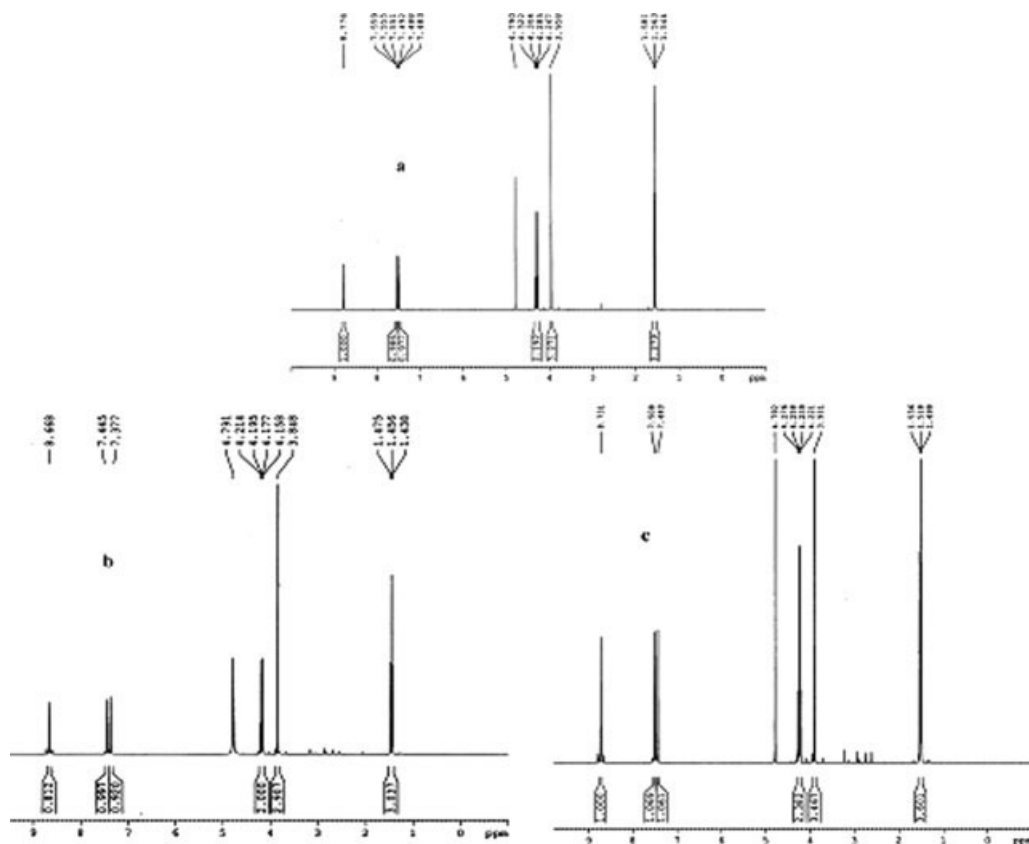


Figure 10. ^1H NMR spectra of EmimBr: (a) freshly made; (b) after first use; (c) after fourth use.

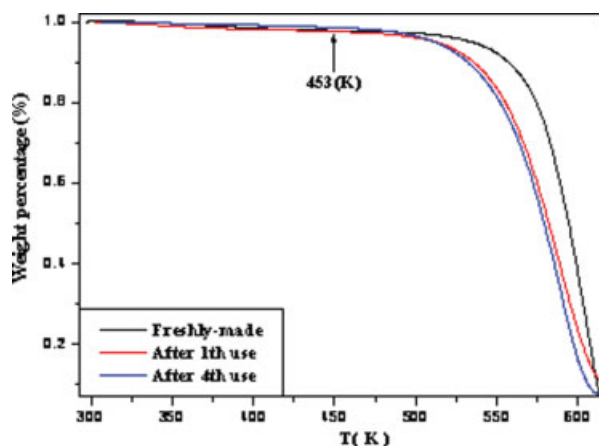


Figure 11. TGA curves of freshly made and used EmimBr ionic liquid.

[Color figure can be viewed in the online issue, which is available at www.interscience.wiley.com.]

water.⁴¹ The introduction of water in reaction is inevitable because of the addition of H_3PO_4 (85% in H_2O) and HF (40% in H_2O). The minim water may affect the content of HF, namely making the control of pH difficult in the system. It is possible that large amounts of HF may break up the imidazolium cation and impair the function of IL as structure-directing agent. Hence the crystal cannot be obtained by using $[\text{Bmim}][\text{PF}_6]$. The similar behavior was also observed by Morris.⁴²

Recycling of IL

The properties of freshly made and recovered EmimBr IL after the reaction was examined using NMR spectroscopy and TGA. Co-substituted aluminophosphate with SOD was selected to explore the recycling of IL by keeping the molar composition to $\text{Al}_2\text{O}_3:5.0\text{P}_2\text{O}_5:3.6\text{HF}:3.0\text{CoCl}_2\cdot6\text{H}_2\text{O}:40$ EmimBr at 453 K for 3 days (Table 1, No. 9). Figure 10 showed the ^1H NMR of the freshly made and used IL, which indicated that there was no obvious change of this EmimBr IL after the first or fourth recycling. To assess the degradation of EmimBr after the reaction, TGA curves of freshly made and used ILs were given in Figure 11. Although there was a little difference at the onset thermal decomposition temperature between the freshly made and used IL, EmimBr was quite stable at the reaction temperature (453 K). And the TGA curves of the first and fourth used IL were almost identical in the entire measurement range. Figure 12 displayed the powder XRD patterns of the Co-substituted aluminophosphate obtained using the freshly made and recycled ILs, and the powder XRD patterns corresponded well with each other. Thus, the IL was not degraded at the reaction temperature and could be recycled. Moreover, there was no change in the structure of the Co-substituted aluminophosphates.

Magnetic property

The powder magnetic susceptibility for Co-substituted aluminophosphate has been measured at a field of 1000 Oe from 5 to 300 K. The χ_M and $\chi_M T$ versus T plots for the

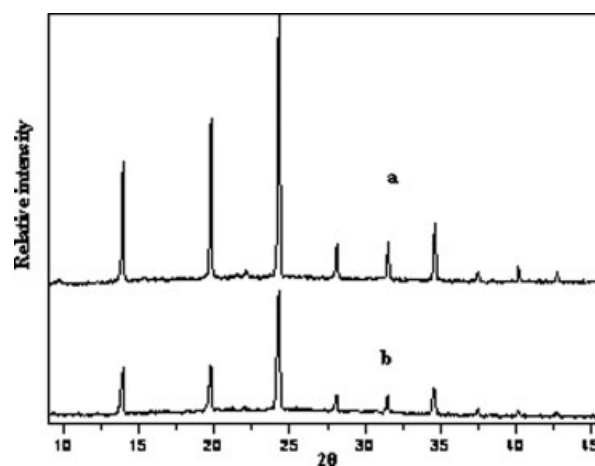


Figure 12. Powder XRD patterns of Co-substituted analogue synthesized using (a) freshly made EmimBr; (b) recycled EmimBr.

compound were shown in Figure 13. Upon cooling, $\chi_M T$ decreased steadily over the range of 300–50 K, and then decreased fast from 50 to 5 K, which should be mainly attributed to the zero-field splitting of Co ions. The magnetic susceptibility of the compound obeys the Curie–Weiss law, with the Weiss constant $\theta = -3.01$ K and the Curie constant $C = 0.822 \text{ m}^3 \text{ mol}^{-1} \text{ K}$ at measured temperature. These results suggested weak antiferromagnetic interactions between Co ions.

Conclusions

Pure and Co (Fe)-substituted aluminophosphates were synthesized ionothermally using imidazolium-based ILs including $[\text{Emim}]\text{Br}$, $[\text{Bmim}]\text{Br}$, and $[\text{Bmim}][\text{BF}_4]$ at near atmospheric pressure without addition of any volatile organic solvents. The powder XRD patterns and FT-IR spectra indicated that all the resulting microporous materials were with SOD structure. The optimum synthesis conditions were found to be at lower concentration of orthophosphoric acid and

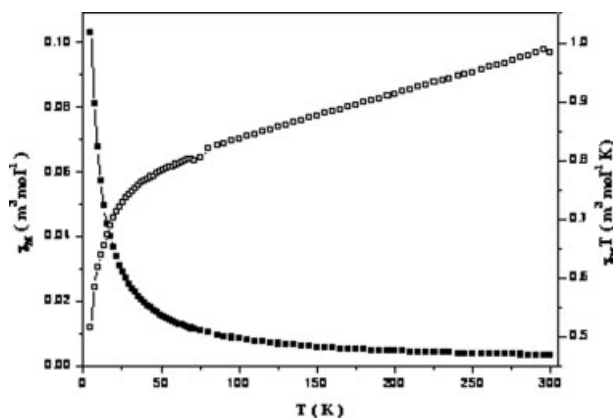


Figure 13. Plots of the temperature dependence of χ_M (■) ($\text{m}^3 \text{ mol}^{-1}$) and $\chi_M T$ (□) ($\text{cm}^3 \text{ mol}^{-1} \text{ K}$) for Co-substituted analogue.

higher temperature in the range of 443–463 K. High product selectivity and large intact crystals were obtained by using ionothermal synthesis under the optimized conditions.

IL could be recycled in ionothermal system and the obtained Co-substituted analogue displayed an antiferromagnetic behavior. EDAX analysis indicated that metal ions successfully substituted sites of Al in the framework at different extents. And it confirmed that the ionothermal synthesis was suitable for preparation of transition metal-incorporated frameworks which were widely applied in a variety of industrial applications such as heterogeneous catalysis, gas adsorption, and separation.

In summary, this work confirms that the novel ionothermal approach is a simple and safe method for synthesis of various microporous molecular sieves, with a number of advantages such as avoiding introduction of volatile organic compounds and allowing the preparation at ambient pressure. And the recycling of IL makes the synthesis of molecular sieves more efficient and environmental. Therefore, it is expected that this new method will become an effective way for large-scale production of molecular sieves and other porous materials in the future.

Acknowledgments

This work was supported financially by the National Natural Science Foundation of China (Grant No. 20436050), the National Science Foundation for Distinguished Young Scholars of China (Grant No. 20625618), and the National 863 Program of China (Grant No. 2006AA06Z376).

Literature Cited

- Davis ME. Ordered porous materials for emerging applications. *Nature*. 2002;417:813–821.
- Rolnick PD, Kobayashi R. Adsorption of methane and several mixtures of methane and carbon dioxide at elevated pressures and near ambient temperatures on 5Å and 13X molecular sieves by tracer perturbation chromatography. *AIChE J*. 1980;26:616–625.
- Huddersman K, Klimczyk M. Separation of branched hexane isomers using zeolite molecular sieves. *AIChE J*. 2004;42:405–408.
- Wilson ST, Lok BM, Messina CA, Cannan TR, Flanigen EM. Aluminophosphate molecular sieves: a new class of microporous crystalline inorganic solids. *J Am Chem Soc*. 1982;104:1146–1147.
- Afewerki M, Dorset DL, Kennedy GJ, Strohmaier KG. Synthesis and characterization of a new microporous material, Part 1: Structure of aluminophosphate EMM-3. *Chem Mater*. 2006;18:1697–1704.
- Barrett PA, Sankar G, Stephenson R, Catlow CRA, Thomas JM, Jones RH, Teat SJ. A new addition to the phillipsite family of molecular sieves: a divalent metal-ion-framework substituted microporous aluminophosphate (DAF-8). *Solid State Sci*. 2006;8:337–341.
- Zhang M, Zhou D, Li JY, Yu JH, Xu J, Deng F, Li GH, Xu RR. Synthesis and characterization of a new layered fluoroaluminophosphate (C₄H₁₁NOH)_{3.5}[Al₄(PO₄)₅F]·0.5H₂O with extra-large 16-rings. *Inorg Chem*. 2007;46:136–140.
- Shi L, Li JY, Duan FZ, Yu JH, Li Y, Xu RR. [C₃N₂H₁₂]₂[MnAl₃P₄O₁₇]₂·[H₃O]: a manganese (II)-substituted aluminophosphate with zeolite AFN topology. *Micropor Mesopor Mater*. 2005;85:252–259.
- Zadrozna G, Sauvage E, Kornatowski J. Characterization of CrAPO-5 materials in test reactions of conversion of 2-methyl-3-butyn-2-ol and isopropanol. *J Catal*. 2002;208:270–275.
- Selvam P, Mohapatra SK. Synthesis and characterization of divalent cobalt-substituted mesoporous aluminophosphate molecular sieves and their application as novel heterogeneous catalysts for the oxidation of cycloalkanes. *J Catal*. 2005;233:276–287.
- Selvam P, Mohapatra SK. Thermally stable trivalent iron-substituted hexagonal mesoporous aluminophosphate (FeHMA) molecular sieves: synthesis, characterization, and catalytic properties. *J Catal*. 2006;238:88–89.
- Saha SK, Waghmode SB, Maekawa H, Kawase R, Komura K, Kubota Y, Sugi Y. Magnesiumaluminophosphate molecular sieves with ATS topology: synthesis by dry-gel conversion method and catalytic properties in the isopropylation of biphenyl. *Micropor Mesopor Mater*. 2005;81:277–287.
- Cooper ER, Andrews CD, Wheatley PS, Webb PB, Wormald P, Morris RE. Ionic liquids and eutectic mixtures as solvent and template in synthesis of zeolite analogues. *Nature*. 2004;430:1012–1016.
- Parnham ER, Wheatley PS, Morris RE. The ionothermal synthesis of SIZ-6-a layered aluminophosphate. *Chem Commun*. 2006;4:380–382.
- Parnham ER, Morris RE. The ionothermal synthesis of cobalt aluminophosphate zeolite frameworks. *J Am Chem Soc*. 2006;128:2204–2205.
- Parnham ER, Morris RE. 1-Alkyl-3-methyl imidazolium bromide ionic liquids in the ionothermal synthesis of aluminium phosphate molecular sieves. *Chem Mater*. 2006;18:4882–4887.
- Parnham ER, Morris RE. Ionothermal synthesis using a hydrophobic ionic liquid as solvent in the preparation of a novel aluminophosphate chain structure. *J Mater Chem*. 2006;16:3682–3684.
- Wang L, Xu YP, Wei Y, Duan JC, Chen AB, Wang BC, Ma HJ, Tian ZJ, Lin LW. Structure-directing role of amines in the ionothermal synthesis. *J Am Chem Soc*. 2006;128:7432–7433.
- Xu YP, Tian ZJ, Wang SJ, Hu Y, Wang L, Wang BC, Ma YC, Hou L, Yu JY, Lin LW. Microwave-enhanced ionothermal synthesis of aluminophosphate molecular sieves. *Angew Chem Int Ed*. 2006;45:3965–3970.
- Seddon KR. Ionic liquids for clean technology. *J Chem Tech Biotechnol*. 1997;68:351–356.
- Weitkamp J, Fritz M, Ernst S. Zeolites as media for hydrogen storage. *Int J Hydrogen Energy*. 1995;20:967–970.
- Van den Berg AWC, Bromley ST, Jansen JC. Thermodynamic limits on hydrogen storage in sodalite framework materials: a molecular mechanics investigation. *Micropor Mesopor Mater*. 2005;78:63–71.
- Paillaud JL, Marichal C, Roux M, Baerlocher C, Chézeau JM. Tripling of the unit cell volume of the non-centrosymmetric AlPO₄-SOD after dehydration: a structural study of a reversible process. *J Phys Chem B*. 2005;109:11893–11899.
- Roux M, Marichal C, Paillaud JL, Fernandez C, Baerlocher C, Chézeau JM. Structural investigation by multinuclear solid state NMR and X-ray diffraction of as-synthesized, dehydrated, and calcined AlPO₄-SOD. *J Phys Chem B*. 2001;105:9083–9092.
- Xu YH, Zhang BG, Chen XF, Liu SH, Duan CY, You XZ. An open framework aluminophosphate with unique 12-membered ring channels: Al₉(PO₄)₁₂(C₂₄H₉₁N₁₆)·17H₂O. *J Solid State Chem*. 1999;145:220–226.
- Loiseau T, Beitone L, Millange F, Taulelle F, O'Hare D, Férey G. Observation and reactivity of the chainlike species ([Al(PO₄)₂]³⁻)_n during the X-ray diffraction investigation of the hydrothermal synthesis of the super-sodalite sodium aluminophosphate MIL-74 (Na₂Al₇(PO₄)₁₂·4tren·H₃O·Na(H₂O)₁₆). *J Phys Chem B*. 2004;108:20020–20029.
- Beitone L, Huguenard C, Gansmüller A, Henry M, Taulelle F, Loiseau T, Férey G. Order-disorder in the super-sodalite Zn₃Al₆(PO₄)₁₂·4tren, 17H₂O (MIL-74): a combined XRD-NMR assessment. *J Am Chem Soc*. 2003;125:9102–9107.
- Beitone L, Loiseau T, Millange F, Huguenard C, Fink G, Taulelle F, Grenèche JM, Férey G. Tetrahedrally coordinated Iron(II) incorporation in the super-sodalite aluminophosphate Fe₃Al₆(PO₄)₁₂·4tren·17H₂O (MIL-74). *Chem Mater*. 2003;15: 4590–4597.
- Loiseau T, Beitone L, Taulelle F, Férey G. Divalent metal incorporation in MIL-74, the super-sodalite aluminum phosphates M₃Al₆(PO₄)₁₂·4tren·17H₂O (M = Mg, Mn, Co) and its gallium phosphate analogs M'₃Ga₆(PO₄)₁₂·4tren·17H₂O (M' = Mg, Mn, Co, Fe, Zn). *Solid State Sci*. 2006;8:346–352.
- Chun S, Dzyuba SV, Bartsch RA. Influence of structural variation in room-temperature ionic liquids on the selectivity and efficiency of competitive alkali metal salt extraction by a crown ether. *Anal Chem*. 2001;73:3737–3741.
- Holbrey JD, Seddon KR. The phase behaviour of 1-alkyl-3-methylimidazolium tetrafluoroborates: ionic liquids and ionic liquid crystals. *J Chem Soc Dalton Trans*. 1999;13:2133–2139.

32. Sheldrick GM. *SHELX-97, PC-version*. Germany: University of Göttingen, 1997.
33. Feng PY, Bu XH, Stucky GD. Hydrothermal synthesis and structural characterization of zeolites analogue compounds based on cobalt phosphate. *Nature*. 1997;388:735–741.
34. Flanigen EM, Lok BM, Patton RL, Wilson ST. Aluminophosphate molecular sieve and the periodic table. New developments zeolite science and technology. In: Murakami, Lijima A, Ward JM, editors. *Proceedings of the seventh International Zeolite Conference*. Amsterdam: Elsevier, 1986;103–112.
35. Hochtl M, Jentys A, Vinek H. Acidity of SAPO and CoAPO molecular sieves and their activity in the hydroisomerization of *n*-heptane. *Micropor Mesopor Mater*. 1999;31:271–285.
36. Dongare MK, Sabde DP, Shaikh RA, Kamble KR, Hegde SG. Synthesis, characterization and catalytic properties of ZrAPO-5. *Catal Today*. 1999;49:267–276.
37. Xu BJ, Han XL, Yan ZF, Zhang ZH. Synthesis, characterization and catalytic properties of CoAPO-11 molecular sieve: skeletal isomerization of 1-hexene. *J Fuel Chem Technol*. 2005;33:617–621.
38. Venkatathri N. Synthesis of AlPO₄-31 from nonaqueous systems. *Mater Lett*. 2003;58:241–244.
39. Jung SH, Hwang YK, Chang JS, Park SE. Effect of acidity and anions on synthesis of AFI molecular sieves in wide pH range of 3–10. *Micropor Mesopor Mater*. 2004;67:151–157.
40. Jiang FY, Zhai JP, Yea JT, Han JR, Tang ZK. Synthesis of large optically clear AlPO₄-5 single crystals. *J Cryst Growth*. 2005;283:108–114.
41. Huddleston JG, Visser AE, Reichert WM, Willauer HD, Broker GA, Rogers RD. Characterization and comparison of hydrophilic and hydrophobic room temperature ionic liquids incorporating the imidazolium cation. *Green Chem*. 2001;3:156–164.
42. Parnham ER, Slawin AMZ, Morris RE. Ionothermal synthesis of β -NH₄AlF₄ and the determination by single crystal X-ray diffraction of its room temperature and low temperature phases. *J Solid State Chem*. 2007;180:49–53.

Manuscript received Jun. 6, 2007, and revision received Sept. 24, 2007.